

INTRODUCTION: 68415 is a fairly homogeneous basaltic impact melt but with a patchy distribution of light and dark colors suggestive of resorbed clasts (Fig. 1). It contains 75-80% plagioclase in an interlocking network, is contaminated with meteoritic siderophiles, and has a precise Rb-Sr age of 3.84 ± 0.01 b.y. (Papanastassiou and Wasserburg, 1972a). The Rb-Sr isotopic data strongly suggest that 68415 was *totally* molten at 3.84 b.y., leaving no relics.

Both 68415 and 68416 were chipped from the top of a 0.5 m angular boulder (Fig. 2) on the outside rim of a 5 m crater. The samples were taken ~20 cm apart. 68415 is greenish-gray, coherent and has many zap pits on its lunar exposed, rounded face.

PETROLOGY: Petrographic descriptions with microprobe analyses are given by Gancarz et al. (1972), Helz and Appleman (1973), Walker et al. (1973) and Vaniman and Papike (1981). A brief description is given by McGee et al. (1979). Nord et al. (1973) report high voltage electron microscope (HVEM) studies of mineral phases, and Takeda



FIGURE 1a. S-72-37346.



FIGURE 1b. S-75-32778.

(1973) gives some microprobe and x-ray data for pyroxenes. Studies of opaque phases, particularly Fe-metal and schreibersite, are reported by L.A. Taylor et al. (1973a), Misra and Taylor (1975), and Pearce et al. (1976). Meyer et al. (1974) report trace element abundances in plagioclases, from ion probe analyses. Studies on crack porosity (Simmons et al., 1974), olivine-augite equilibration temperature (Ridley and Adams, 1976) and ilmenite paragenesis (Englehardt, 1978, 1979) have been reported. Jagodzinski and Korekawa (1973) studied diffuse x-ray scattering of plagioclases, mainly to understand radiation defects. Hewins and Goldstein (1975a) modeled the metal compositions reported by L.A. Taylor et al. (1973a) using fractional crystallization schemes.

68415 has an ophitic-subophitic texture with a few phenocrysts (Fig. 3); although some authors have referred to the texture as intersertal, there is so little glass (<1%) that the term is inappropriate. According to Helz and Appleman (1973) the grain size is seriate, with rare phenocrysts. The dominant texture is of interlocking plagioclase laths with interstitial mafic minerals, but grades to phenocryst-like plagioclase, sometimes in radial

clusters, and fine-grained patches which are possibly cognate inclusions (Gancarz et al., 1972). Neither Walker et al. (1973) nor Helz and Appleman (1973) observed obvious xenocrystic plagioclase and suggest that there is little accumulated plagioclase; in contrast Gancarz et al. (1972) suggest that the sample contains 5 to 25% accumulated plagioclase. While Helz and Appleman (1973) and Walker et al. (1973) suggest that an impact melt origin is most likely, Gancarz et al. (1972) leave open the possibility of a partial melt of a source even more aluminous than 68415 itself.

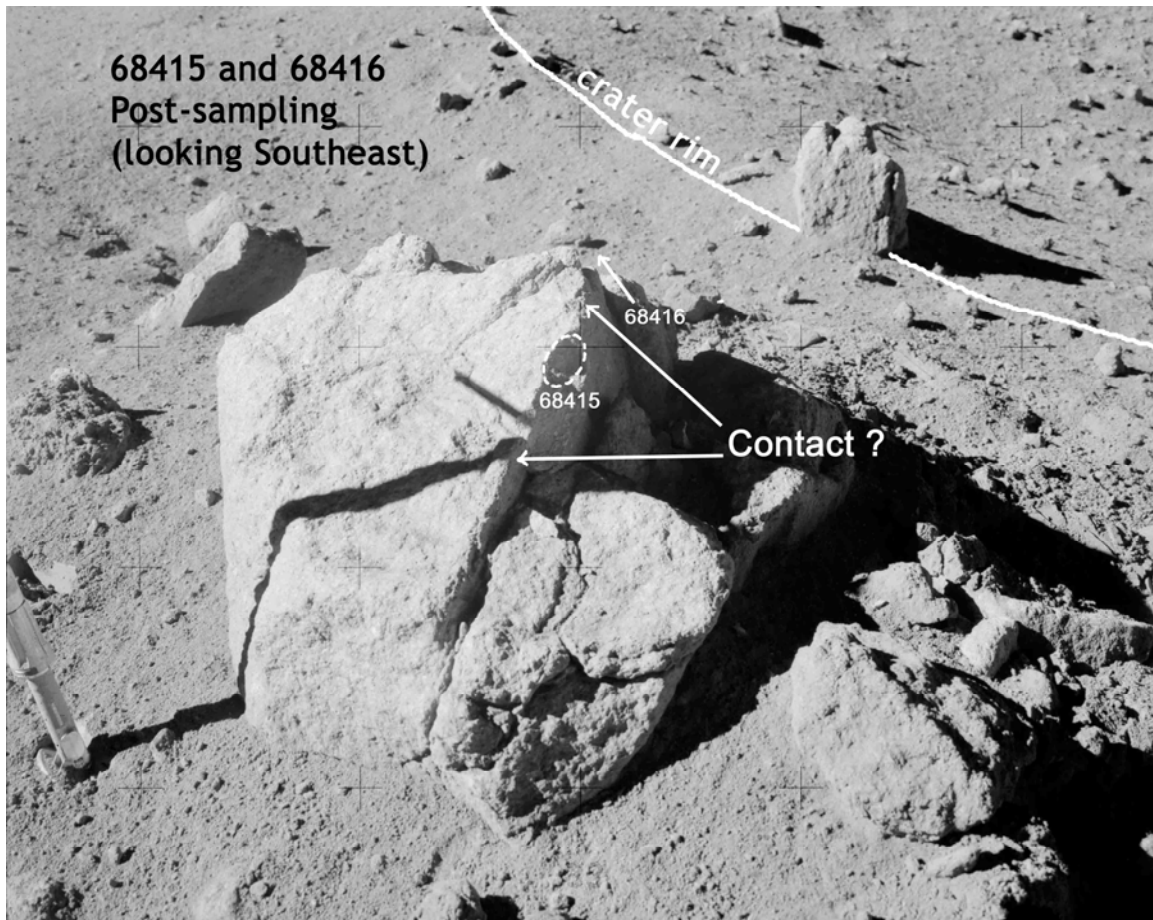


FIGURE 2. AS16-108-17698.

Groundmass plagioclases are mainly An_{98-92} , but rims range to An_{71} (Fig. 4). The phenocrysts and large grains have cores with the same compositions as the groundmass and the large grains frequently show a reversal of zoning at their outer edges (Gancarz et al., 1972; Helz and Appleman, 1973; Walker et al., 1973). Nord et al. (1973) detail antiphase domains in plagioclase. Meyer et al. (1974) show that plagioclases do not differ significantly in their trace element contents (Table 1), thus there is no evidence that any of the plagioclases they analyzed are relict. The interiors of grains are chemically homogeneous. Pyroxenes show two main compositional clusters, of which low-Ca varieties are dominant (Fig. 5). Orthopyroxene is not present. Pyroxenes are zoned, but not in any systematic fashion, although the most iron-rich grains occur only in mesostasis

regions. Exsolution is not apparent with the petrographic microscope, but Nord et al. (1973) observed 1000 Å wide augite lamellae in pigeonite, using HVEM techniques, and Takeda (1973) also found x-ray evidence for augite exsolution. The small, interstitial olivine crystals have restricted compositions with the total reported range of Fo₆₇₋₇₃. Ridley and Adams (1976) calculated an olivine-augite equilibration temperature of 998°C.



FIGURE 3. a) 68415,133, xpl. Width 2 mm.
b) 68415,141, xpl. Width 2 mm.

TABLE 1. Ion microprobe data for trace elements in 68415,131 (from Meyer et al., 1974) (wt% and ppm).

	# analyses	Na ₂ O	Li	Mg	K	Ti	Sr	Ba
Large grains	27	0.29	1.5	790	110	75	177	11
Small grains	3	0.22	1.0	490	55	83	180	17
Grain A	4	0.31	1.8	570	100	68	192	13
Grain B	6	0.27	1.5	680	71	62	188	11

The mode by Gancarz et al. (1972) has 82% plagioclase, 8% pigeonite, 4% augite, 3% olivine ~2% mesostasis (~1% ilmenite, chromite, ulvospinel, troilite, Fe-metal, cristobalite, and glass). Other modes are fairly similar, differing mainly in the plagioclase and olivine contents. Other phases observed include armalcolite (Helz and Appleman, 1973), schreibersite (Misra and Taylor, 1975 and others), and phosphates and Y-Zr phases (Anderson and Hinthorne, 1973).

Metal grains have compositions spanning a wide range (Fig. 6) (Gancarz et al., 1972; L.A. Taylor et al., 1973a; Misra and Taylor, 1975; Pearce et al., 1976), and appears to have formed throughout the crystallization sequence, occurring in large plagioclases through to mesostasis areas. Schreibersite is fairly common in metal-schreibersite-troilite particles (less than 20 μm in diameter) enclosed in plagioclase; the compositions of coexisting metal and troilite suggest an equilibration temperature of $\sim 650^\circ\text{C}$ (Misra and Taylor, 1975). Residual, mesostasis glasses contain 64-85% SiO_2 and 0.2-5.0% K_2O (Gancarz et al., 1972). Anderson and Hinthorne (1973) report ion-probe analyses of rare earth elements in a Y-Zr phase and phosphates, as well as Th/U ratios.

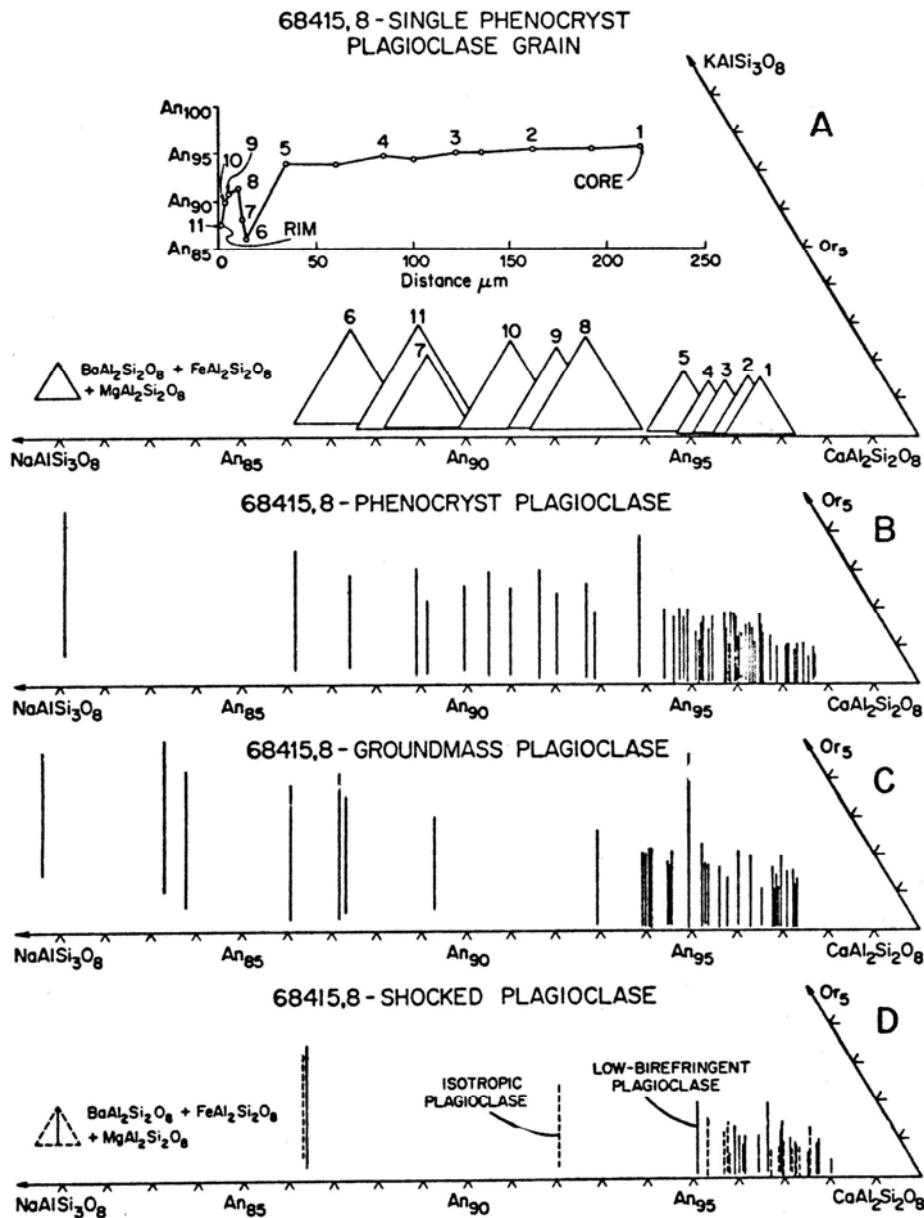


FIGURE 4. Plagioclase compositions; from Gancarz et al. (1972).

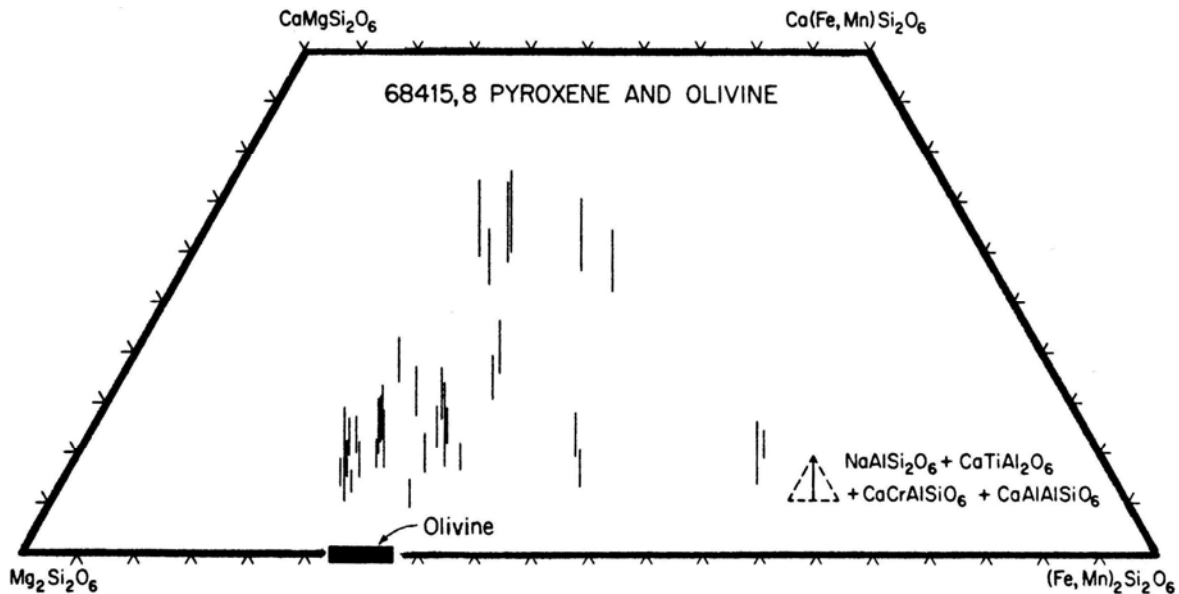


FIGURE 5. Mafic mineral compositions; from Gancarz et al. (1972).

EXPERIMENTAL PETROLOGY: Results of phase equilibria studies are reported by Walker et al. (1973), Ford et al. (1974), and Muan et al. (1974).

Walker et al. (1973) conducted crystallization experiments on a 68415 composition at several pressures (Fig. 7). The composition is not related to any low pressure saturation curves. If the composition was a result of partial melting, the experiments suggest that the source would have consisted of anorthite+spinel+corundum at 18 kb. Such a lunar interior is unlikely, and Walker et al. (1973) prefer to interpret 68415 as a total impact melt. Ford et al. (1974) conducted atmospheric pressure experiments; plagioclase is the liquidus phase followed by spinel, which is not, however, stable below the solidus. They state that high water pressure suppresses plagioclase and that a water pressure over 5 kb would cause olivine to be the liquidus phase, and suggest that 68415 could have been produced by partial melting under high water pressure in the lunar interior. Muan et al. (1974) briefly report on low-pressure equilibrium experiments on 68415. The sequence of crystallization with decreasing pressure is plagioclase, spinel, olivine. Olivine, pyroxene and plagioclase coexist with liquid at some unspecified temperature between 1080°C and 1150°C.

CHEMISTRY: A list of references to chemical work is given in Table 2, a summary chemical composition in Table 3, and rare-earth element abundances in Figure 8.

Few of the references contain much specific discussion. The rock is both more aluminous and poorer in incompatible elements, transition metals, and volatile elements than local soils. Philpotts et al. (1973) remark on the homogeneity of the sample at the 0.1 g level; the REE abundances shown in Figure 8 for ,79 is for two near-identical

compositions. The level of siderophiles (Krahenbuhl et al., 1973; Wasson et al., 1975) demonstrates significant meteoritic contamination. The meteoritic signature was classed DN by Ganapathy et al. (1973), Group 2 by Gros et al. (1976), and eventually considered (unreliably) Group 1H and possibly hybridized by Hertogen et al. (1977).

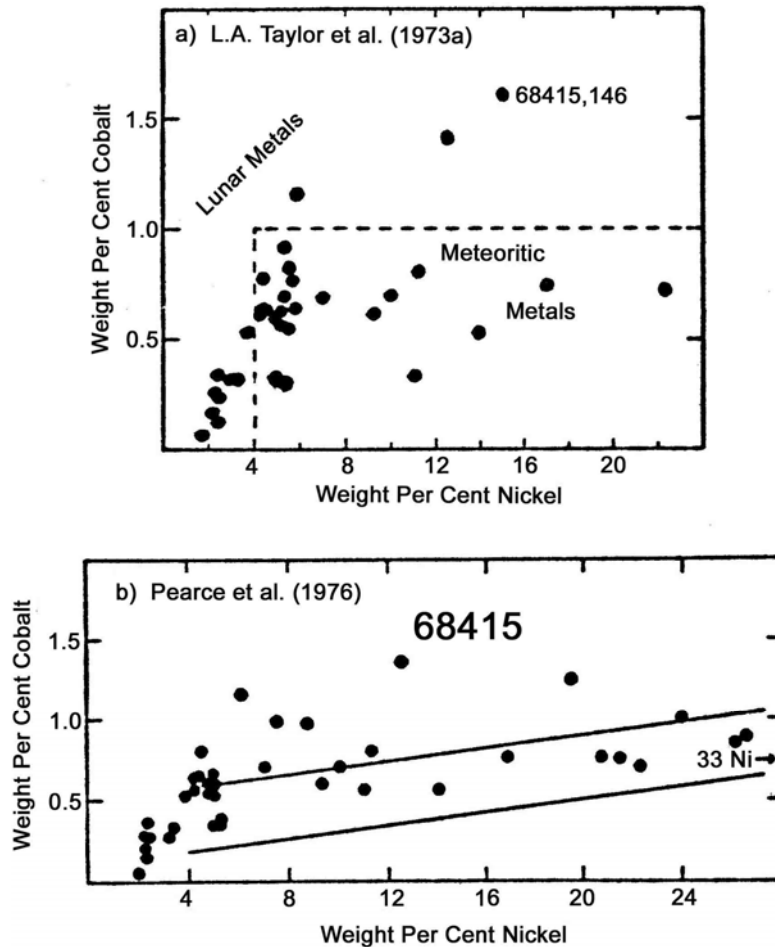


FIGURE 6. Metals.

STABLE ISOTOPES: Clayton et al. (1973) analyzed ,75 for oxygen isotopes. Typical lunar values for δO^{18} ‰ for plagioclase (+5.69) and olivine (+4.91) indicate equilibration at about 1100°C. Taylor and Epstein (1973) found that ,74 whole rock had δSi^{30} ‰ of $+6.08 \pm 0.06$ (two determinations) which, when adjusted for interlaboratory bias, is similar to the Clayton et al. (1973) plagioclase value. The whole rock δSi^{30} of 0.05 ± 0.02 (two determinations) is also fairly typical for lunar samples (Taylor and Epstein, 1973).

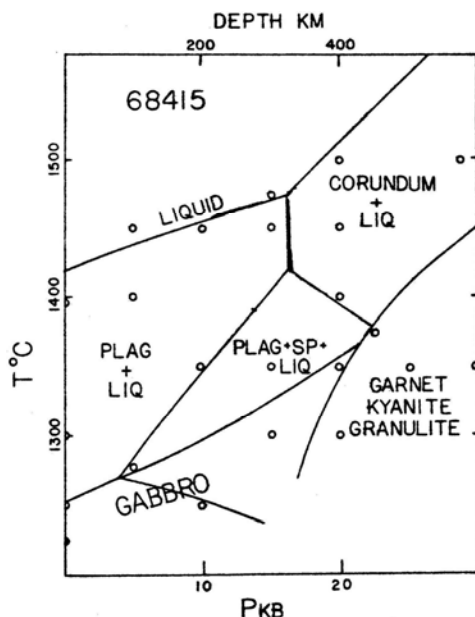


FIGURE 7. Experimental results; from Walker et al. (1973).

GEOCHRONOLOGY: Papanastassiou and Wasserburg (1972a) report a Rb-Sr internal isochron for interior chips (without saw cuts) from ,10 (Fig. 9). A precise age of 3.84 ± 0.01 b.y. with initial $^{87}\text{Sr}/^{86}\text{Sr}$ of 0.69920 ± 3 was obtained. Mineral separations were made using both heavy liquids and a Frantz separator; the whole-rock chip was not contaminated. The initial $^{87}\text{Sr}/^{86}\text{Sr}$ is quite primitive. The T_{BABI} model age of 4.3 ± 0.2 b.y. calculated by Papanastassiou and Wasserburg (1972a) is similar to that calculated from whole-rock data for a second split of ,10 analyzed by Nyquist et al. (1973), 4.44 ± 0.20 b.y.

^{40}Ar - ^{39}Ar data are presented by Stettler et al. (1973), Huneke et al. (1973 and Kirsten et al. (1973) and their release diagrams are shown in Figure 10. The derived ages are summarized in Table 4. These ages are consistent with the internal Rb-Sr isochron age except for that of the plagioclase separate (Huneke et al., 1973). This plagioclase separate is unusual in that its apparent age is greater than that of the whole rock, the reverse of the results usually obtained from lunar rocks. This feature is not understood (Huneke et al., 1973).

Nunes et al. (1973) report whole rock U, Th, and Pb isotopic data. These fall on concordia at 4.47 b.y. and, by definition, also on a 3.99 to 4.47 b.y. discordia line. These data cannot by themselves specify the crystallization age. Tera et al. (1973) report U, Th, and Pb isotopic data for bulk rock and mineral separates. The large difference in $^{207}\text{Pb}/^{206}\text{Pb}$ between the bulk rock and the plagioclase separate shows that there is initial radiogenic Pb in the rock. Thus the essentially concordant whole rock U-Th-Pb ages of 4.47 b.y. do not correspond to the crystallization age but reflect the possibility that the rock was an early lunar differentiate, not significantly altered isotopically during its

melting at ~3.9 b.y. An isochron through the plagioclase and whole rock data intersect concordia at 3.94 ± 0.05 and 4.47 ± 0.02 b.y. (Fig. 11, where the isochron drawn is for combined 65015 and 68415 data). In Tera et al. (1974) the same data are presented but with more discussion. The whole-rock concordant age is revised down to 4.42 b.y. because of the use of different U decay constants, but the main conclusions are the same as those of Tera et al. (1973).

TABLE 2. Chemical work on 68415.

<u>Reference</u>	<u>Split #</u>	<u>Elements Analyzed</u>
Rose <u>et al.</u> (1973)	,85	Majors, some trace
LSPET (1973)	,6	Majors, some trace
Bansal <u>et al.</u> (1972) } Hubbard <u>et al.</u> (1974) }	,10	Majors, REEs, other trace
Philpotts <u>et al.</u> (1973)	,79	*REEs, other incompatibles
Nava (1974)	,79	Majors
Jovanovic and Reed (1973)	,107	Halogens, Li, U
Krähnenbühl <u>et al.</u> (1973)	,67	Meteoritic siderophiles and volatiles
Jovanovic and Reed (1976a)	,26	Ru, Os
Wasson <u>et al.</u> (1975)	,68	**Meteoritic siderophiles and volatiles
Jovanovic and Reed (1977)	,26	Hg
Reed <u>et al.</u> (1977)	,26	Tl and Zn (volatilized)
Papanastassiou and Wasserburg (1972a)	,10	Rb, Sr, K, Ba
Nyquist <u>et al.</u> (1973)	,10	Rb, Sr
Nunes <u>et al.</u> (1973)	,63	U, Th, Pb
Tera <u>et al.</u> (1973, 1974)	,10	U, Th, Pb
Stettler <u>et al.</u> (1973)	,49	K, Ca
Huneke <u>et al.</u> (1973)	,10	K, Ca
Kirsten <u>et al.</u> (1973)	,50	K, Ca
Rancitelli <u>et al.</u> (1973b)	,1	K, U, Th
Drozd <u>et al.</u> (1974)	?	U

*includes pyroxene and plagioclase as well as two whole-rock replicates

**three replicates

Anderson and Hinthorne report $^{207}\text{Pb}/^{206}\text{Pb}$ ages of 3.96 ± 0.18 b.y. for a phosphate and 3.96 ± 0.28 b.y. for a Zr-phase in 68415. The isotopic data were acquired with the ion probe.

RARE GASES AND EXPOSURE AGES: Ar isotopic data are reported by Stettler et al. (1973), Huneke et al. (1973) and Kirsten et al. (1973), with calculated ^{38}Ar exposure ages of 90 m.y., 105 ± 15 m.y., and 88 ± 4 m.y., respectively for whole rock data. Huneke et al. (1973) also calculated an exposure age of 95 ± 15 m.y. for a plagioclase separate.

Drozd et al. (1974) report Kr isotopic and spallation spectra for whole rock, and calculate an $^{81}\text{Kr-Kr}$ exposure age of 92.5 ± 5.9 m.y., as well as ^{21}Ne (32.5 ± 7.8 m.y.) and ^{38}Ar (113.0 ± 42.0 m.y.) ages. Because the cosmic ray track ages (below) are of the order of a few million years, Drozd et al. (1974) conclude that the rare gas data indicate a pre-surface exposure for 68415.

TABLE 3. Summary chemistry of 68415.

SiO_2	45.5	Sr	180
TiO_2	0.31	La	6.8
Al_2O_3	28.6	Lu	0.3
Cr_2O_3	0.1	Rb	1.7
FeO	4.1	Sc	8.2
MnO	0.05	Ni	~135
MgO	4.4	Co	11
CaO	16.3	Ir ppb	~5
Na_2O	0.48	Au ppb	2.65
K_2O	0.07	C	
P_2O_5	0.07	N	
		S	400
		Zn	1.5
		Cu	12

Oxides in wt%; others in ppm except as noted.

Behrmann et al. (1973), from single point cosmic ray track studies, conclude that 68415 resided at the surface for ~4 m.y. (this data quoted by Crozaz et al., 1974, as Yuhas, unpublished). The cosmogenic radionuclide data of Rancitelli et al. (1973a) shows that ^{26}Al is saturated (Yokoyama et al., 1974) demonstrating a surface exposure of at least a few million years. Morrison et al. (1973) suggest a surface exposure age of ~2 m.y. from microcrater abundances.

MICROCRATERS: Morrison et al. (1973) and Neukum et al. (1973) present frequency v. diameter data for microcraters (Fig. 12). While the crater population is probably in production, the data are not definitive. Morrison et al. (1973) and Neukum et al. (1973) also tabulate data on the diameter of the spall zone/diameter of the pit (D_s/D_p) for both N and S surfaces. Horz et al. (1974) note the considerable overlap of microcraters, hence calculated production rates are minima (Horz et al., 1974 erroneously state that the cosmic ray track and $^{81}\text{Kr-Kr}$ exposure ages are concordant).

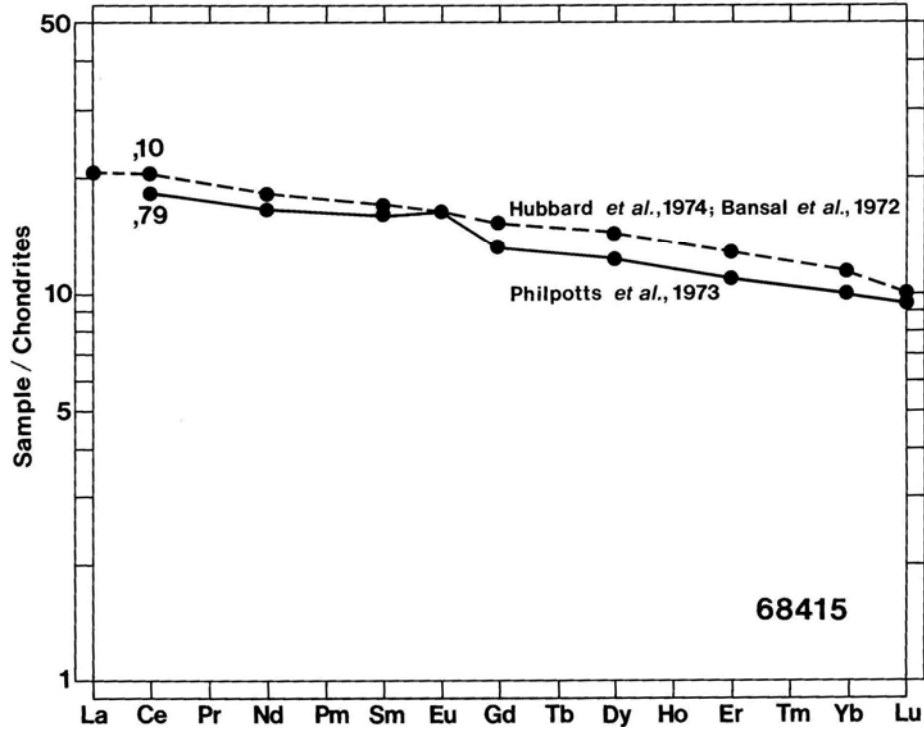


FIGURE 8. Rare earths.

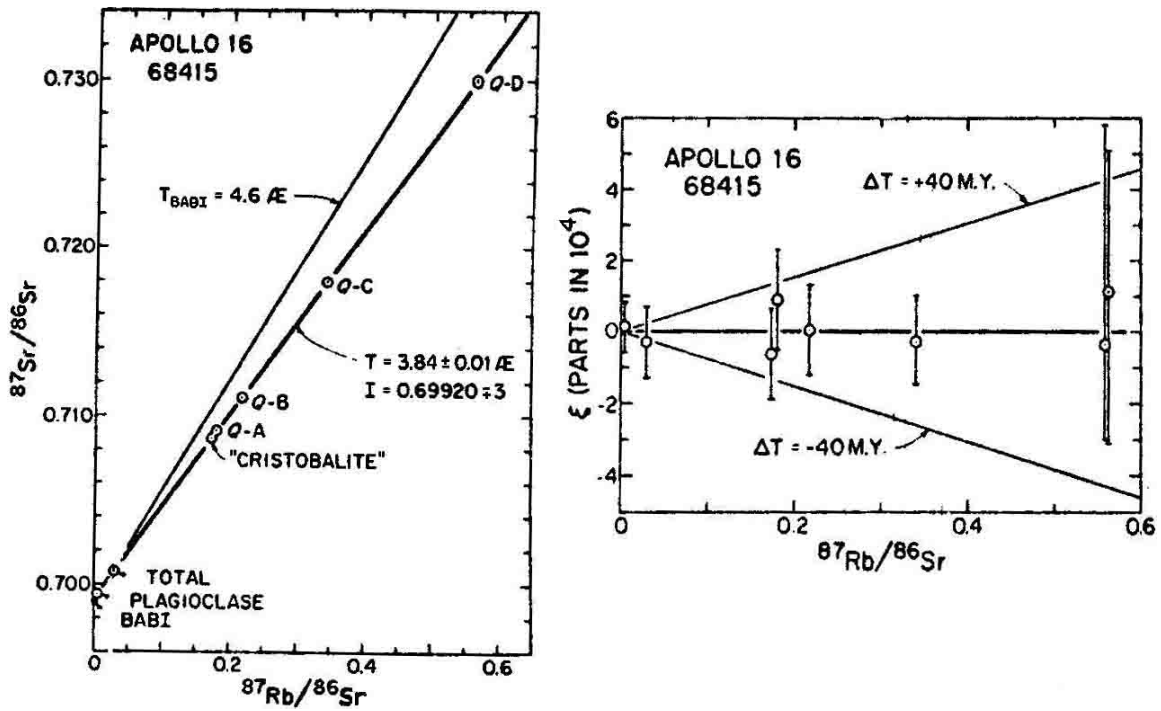


FIGURE 9. Rb-Sr data; from Papanastassiou and Wasserburg (1972a).

PHYSICAL PROPERTIES: Nagata et al. (1973) and Pearce et al. (1973) tabulate basic magnetic properties for bulk rock samples. The results are not in agreement, showing the rock to be magnetically inhomogeneous compared with other lunar crystalline rocks such as mare basalts. Nagata et al. (1973) illustrate the thermal hysteresis of the thermomagnetic curve and demonstrate its inversion into four components (Fig. 13). The cooling curve (of thermomagnetic curve) is more complicated than for other Apollo 16 rocks, having at least three transition points (395°C, 682°C, 781°C) and the heating curve also appears to have at least two transition points (700°C, 781°C). Nagata et al. (1973) tabulate coercive force v. temperature, coercive force, saturation remanent magnetization, saturation magnetization (at 4.2°K and 300°K), and the natural remanent magnetization (NRM) and its stability against alternating field demagnetization. Nagata et al. (1975) discuss some of these data.

Pearce et al. (1973) illustrate the demagnetization of two chips (Fig. 14) which are quite different. ,41 is stable whereas ,17 has a pronounced soft component whose direction is different from that of the stable direction, which is the same in both chips. They note that the results are more appropriate for a recrystallized breccia than for an igneous rock. Pearce et al. (1976) report partial thermoremanent magnetization (PTRM) and NRM for these same two chips ,41 and ,17 as part of a study of the complexities involved in determining lunar paleointensities; the results are shown on several diagrams in their paper. There appears to be no textural control on the magnetic features and the NRM is of thermal origin. ,41 has no stable NRM after alternating field demagnetization to 400 Oe, and the data are not of use for paleointensity determinations. In contrast ,17 gives an ancient field value of ~5000γ, which is substantially lower than the value given for 68416 (from the same boulder) by Stephenson et al. (1974). Pearce and Simonds (1974) tabulate iron valences and iron metal contents deduced from magnetic measurements.

Brecher (1977) found the NRM of chip ,54 to be rather weak but unusually stable in both intensity and direction. The NRM directions lie close to and between two prominent petrographic planes, contrary to the conclusions of Pearce et al. (1976) for chips ,41 and ,17.

Mossbauer spectral analyses for 68415 both “as-received” and annealed at ≥800°C in a He-H₂ atmosphere are reported by Schwerer et al. (1973). The “as received” conditions suggest an absence of metallic iron. Huffman et al. (1974) report the same data and note the difference of metal content as compared to magnetic results, a difference they attribute to sample inhomogeneity.

TABLE 4. Summary of ⁴⁹Ar-³⁹Ar ages (b.y.).

Stettler <i>et al.</i> (1973)	Whole rock	: 3.70±0.10 (plateau), 3.80±0.04 (intermediate release)
Huneke <i>et al.</i> (1973)	Whole rock	: 3.85±0.04 (intermediate release)
	Plagioclase	: 4.09 (intermediate release), 4.51 (final release)
Kirsten <i>et al.</i> (1973)	Whole rock	: 3.85±0.06 (plateau)

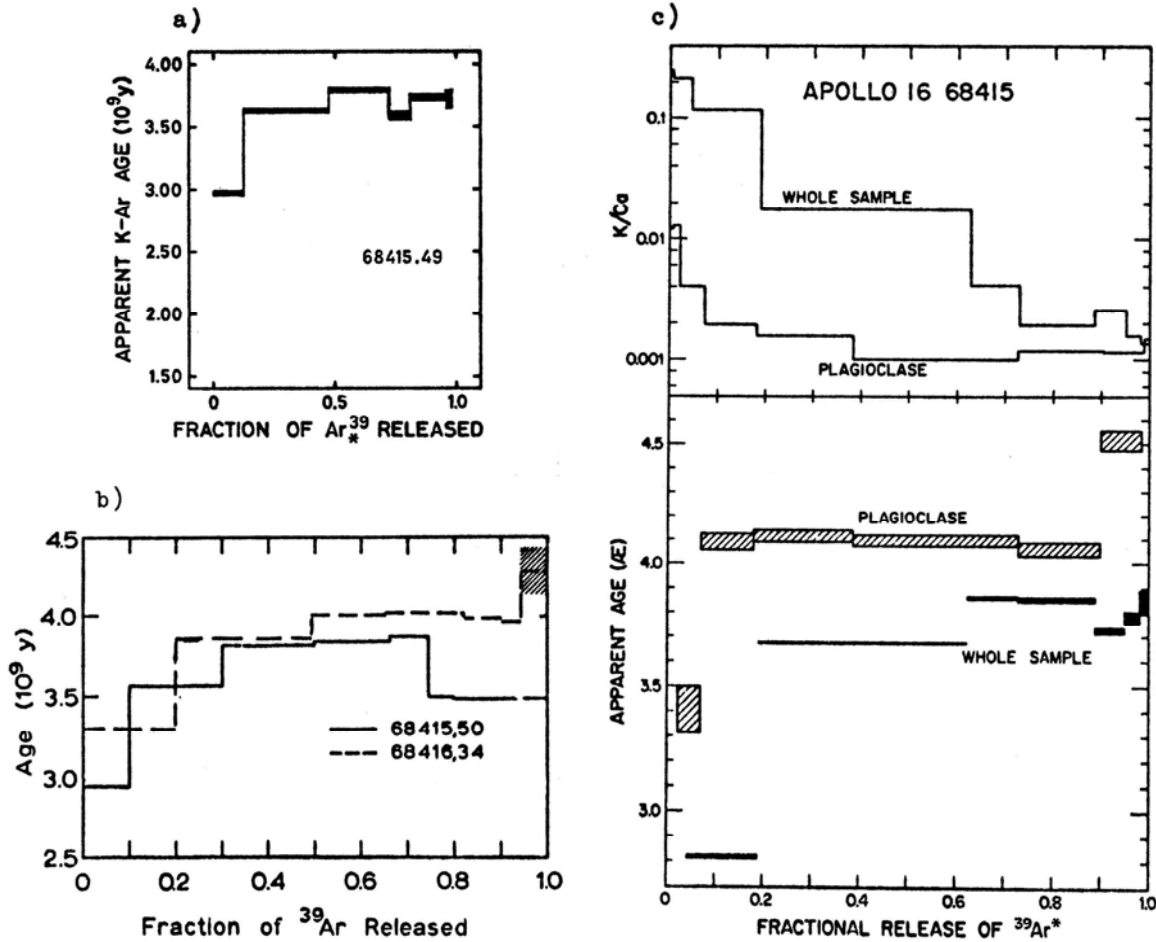


FIGURE 10. Ar release; from a) Kirsten et al. (1973).
 b) Stettler et al. (1973). c) Huneke et al.(1973).

Electrical conductivity measurements are reported by Schwerer et al. (1974). The trend of conductivity v. temperature has an unusual break at low temperatures (Fig. 15) which is reproducible but not well understood.

Todd et al. (1973) measured several physical properties, including elastic wave velocities, density, and crack porosity for ,54 (Table 5), as well as thermal expansion coefficients. They also plot the ratio of the wave velocities at atmospheric pressure and at 10 kb against the crack porosity. Maxwell (1978) used Todd et al.'s (1973) data to calculate Lamé elastic constants. Wang et al. (1973) report the same velocity data as Todd et al. (1973).

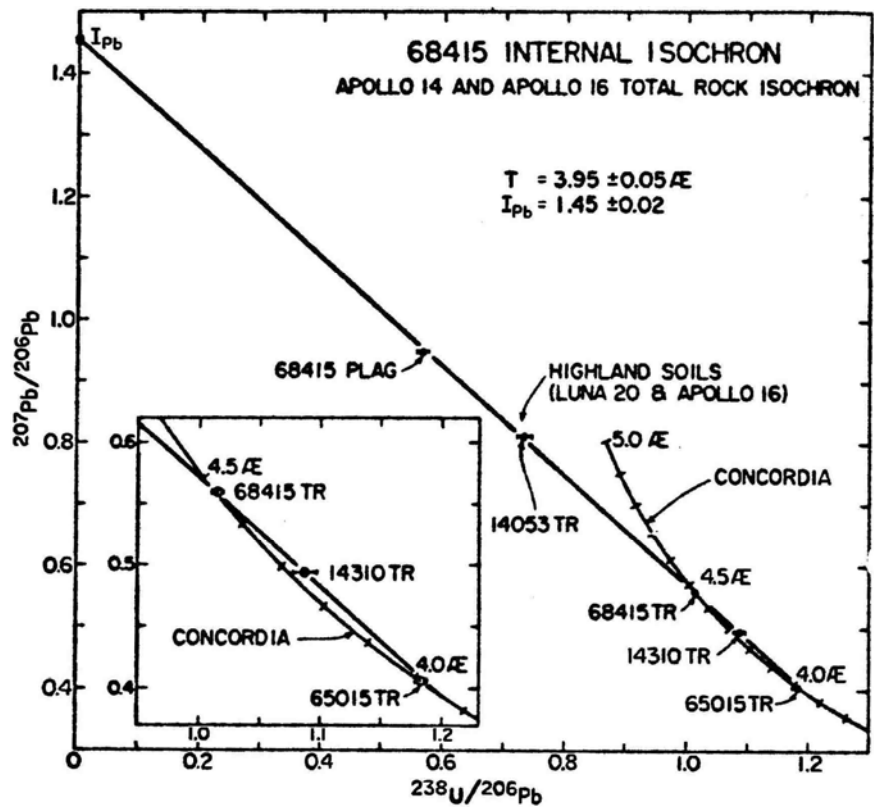


FIGURE 11. U-Pb isochron; from Tera et al. (1973).

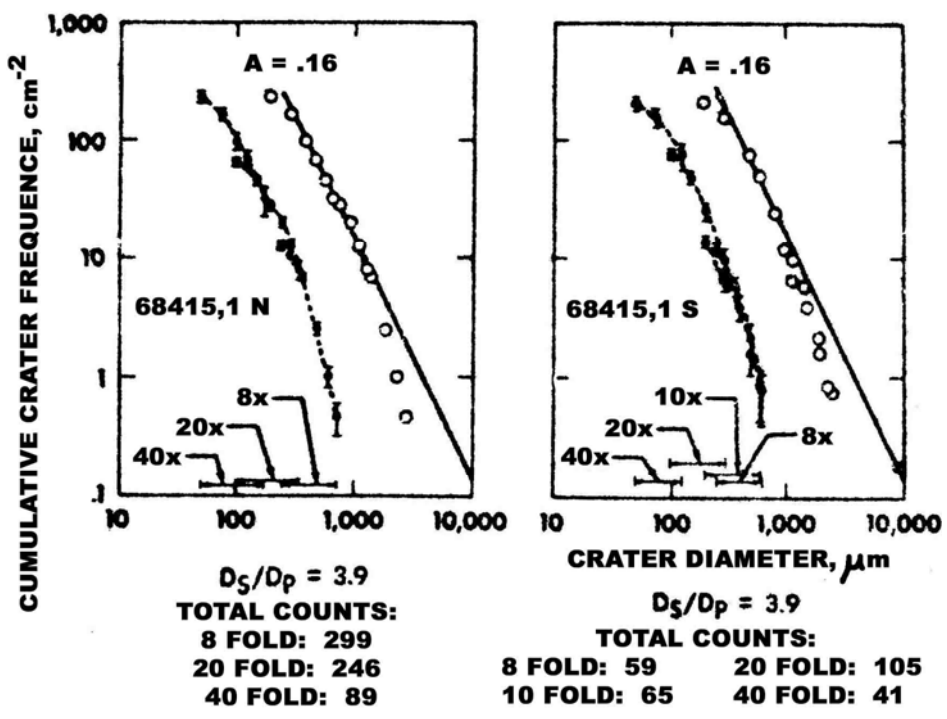


FIGURE 12. Microcraters; from Neukum et al. (1973).

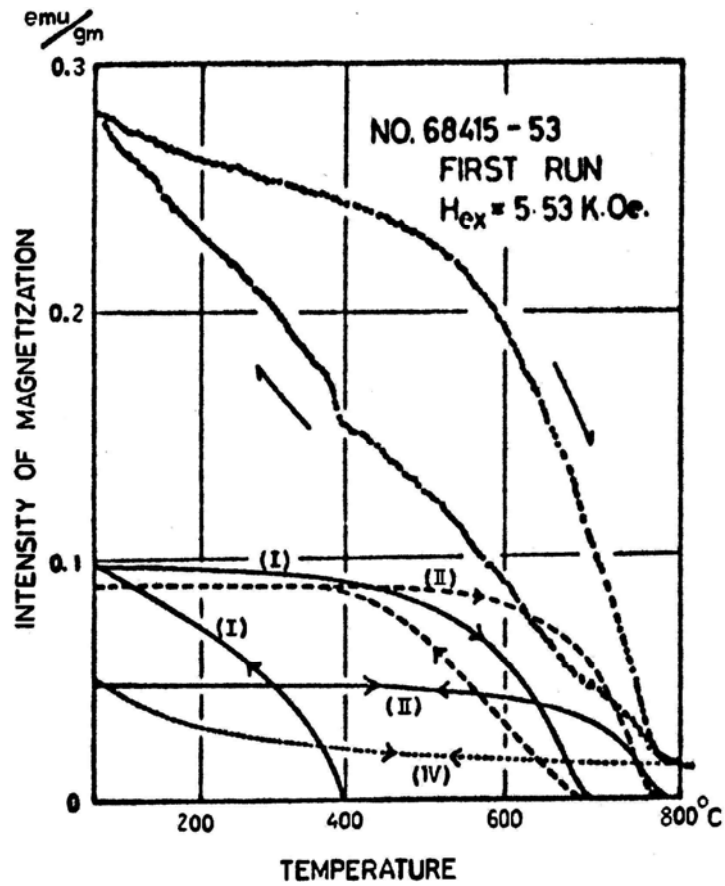


FIGURE 13. Thermal hysteresis; from Nagata et al. (1973).

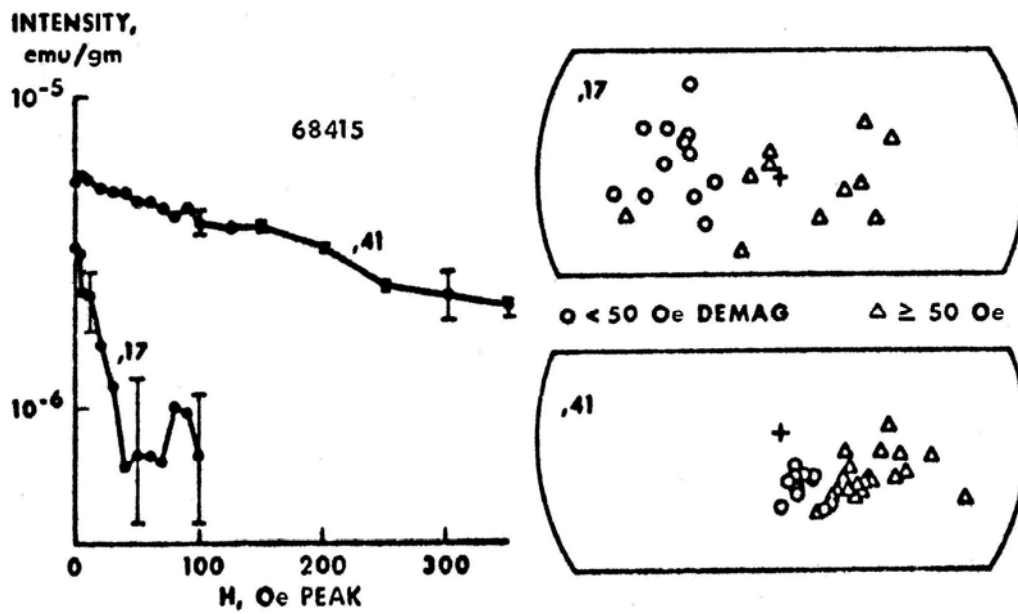


FIGURE 14. Demagnetization; from Pearce et al. (1973).

PROCESSING AND SUBDIVISIONS: 68415 was received as two pieces labeled ,1 (202 g) and ,2 (169 g) both of which were subsequently totally subdivided with several saw cuts (Fig. 16). The largest pieces now remaining are ,30 (113g); ,163 (85g); and ,164 (78g). All other pieces are less than 7 g.

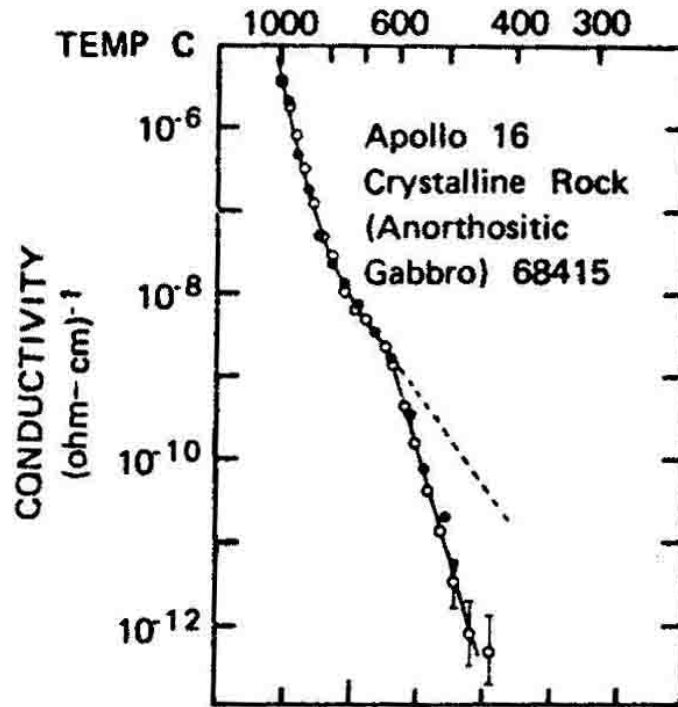


FIGURE 15. Electrical conductivity v. Temperature; from Schwerer et al. (1974).

TABLE 5. Physical properties of 68415,54 (Todd et al., 1973).

				Confining Pressure (bars)										
	Density (g/cc)	Crack Porosity	Elastic Property*	1	100	250	500	750	1000	1500	2000	3000	4000	5000
A direction	2.78	0.83	P	4.70	5.02	5.29	5.63	5.89	6.09	6.37	6.54	6.76	6.85	6.94
			S	2.59	2.69	2.80	2.94	3.05	3.13	3.26	3.35	3.43	3.47	3.54
			β	22.0	15.2	11.1	7.7	5.8	4.7	3.8	3.4	2.7	2.6	2.5
B direction			P	4.95	5.25	5.57	5.92	6.11	6.27	6.49	6.64	6.80	6.92	7.04
			S	2.48	2.60	2.73	2.88	3.00	3.09	3.23	3.31	3.41	3.46	3.54

* P = compressional velocity (km/sec), S = shear velocity (km/sec), β = static compressibility (Mb^{-1}). A and B are mutually perpendicular.

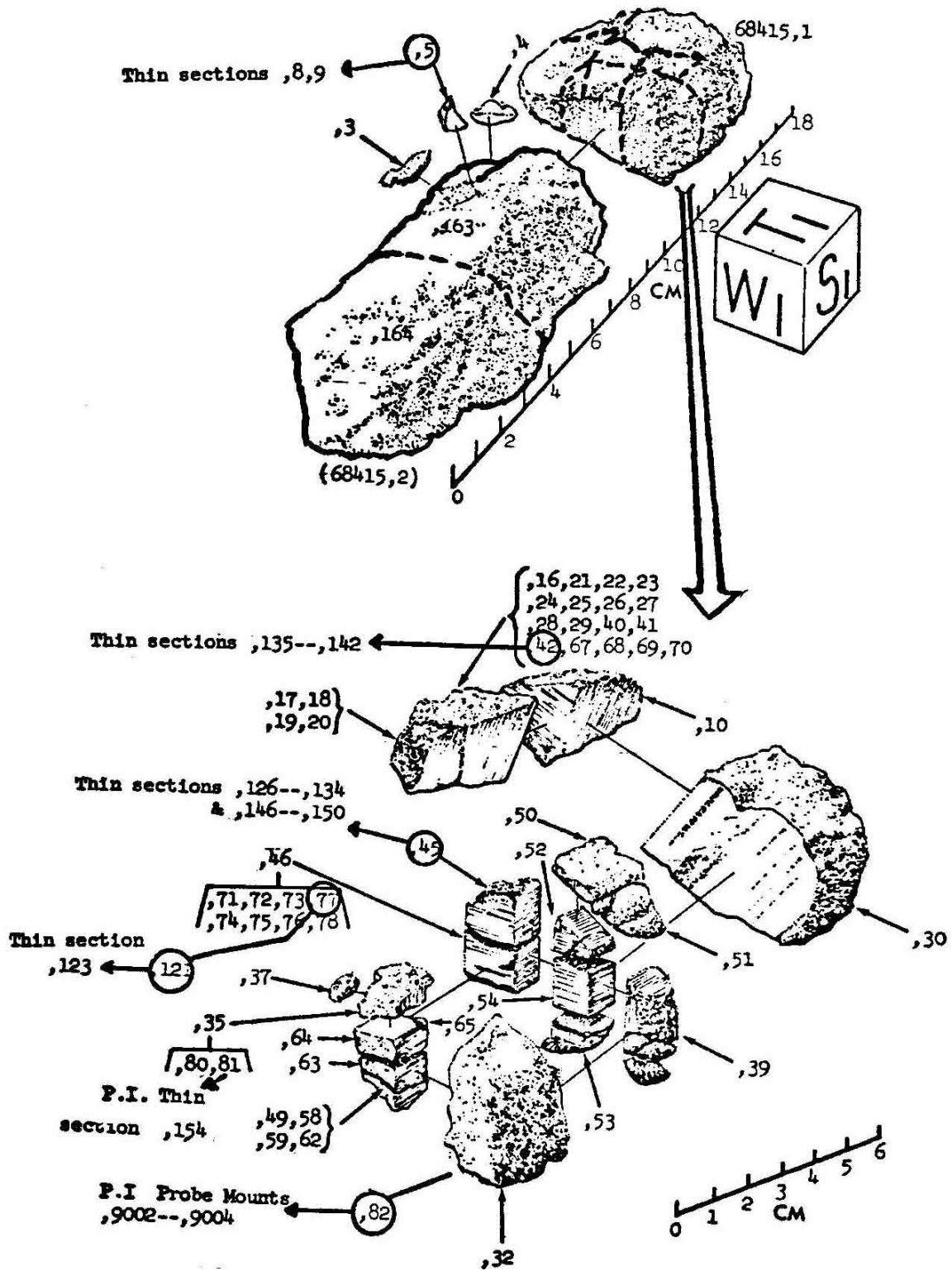


FIGURE 16. Cutting diagram.